Thomson scattering from laser wakefield accelerators

Article · December 2004

DOI: 10.1063/1.1842569

6 authors, including:

Csaba Toth
Lawrence Berkeley National Laboratory

Wim Leemans
Lawrence Berkeley National Laboratory

Thomson scattering from laser wakefield accelerators

Pierre Michel[*], Eric Esarey[*], Carl B. Schroeder[*], Csaba Tóth[*], Wim P. Leemans[*] and Dieter Schneider[†]

[*]*Center for Beam Physics, Lawrence Berkeley National Laboratory, Berkeley, CA 94720, USA*
[†]*Lawrence Livermore National Laboratory, Livermore, CA 94550, USA*

Abstract. The production of ultrashort (fs) x-ray pulses through Thomson scattering of high power laser pulses off relativistic electron bunches generated by laser-plasma accelerators is discussed. These accelerators can typically produce two types of electron bunches: i) a high charge bunch with a broad energy distribution, resulting in x-ray pulses with high flux and a broadband spectrum, and ii) electron bunches with a narrow energy distribution, resulting in an ultrashort x-ray pulse with a nearly monochromatic spectrum. Nonlinear Thomson scattering (high laser intensity) will be considered, as well as the effects of the laser pulse profile. Thomson scattering may provide a useful diagnostic for determining the electron bunch properties via the scattering x-ray spectrum.

INTRODUCTION

There have been a number of tremendous achievements over the past decade in the field of ultrafast x-ray science. One technique to produce short pulses of x-ray light is Thomson scattering of an intense laser off an electron beam. Less than ten years ago, 90^0 Thomson scattering experiments using a femtosecond laser and a RF linac have demonstrated the first production of 30 keV radiation in $\simeq 300$ fs pulses [1]. In addition to being a very promising ultrashort x-ray source, these experiments demonstrated Thomson scattering as a useful tool to probe electron beams [2].

In the following, we discuss the possibility of Thomson scattering off laser-accelerated electrons. It is well known that the fields generated from laser accelerators are much higher than those achievable from standard radiofrequency cavities, as a plasma can sustain fields up to three orders of magnitudes higher [3]. So far the electron bunches produced by laser accelerators were characterized by an exponentially decreasing energy distribution function, up to a few tens of MeV. However, recent experimental techniques such as colliding pulse injection [4–6] might lead to the production of quasi-monoenergetic electron beams from laser-plasma accelerators in a near future.

The narrow and exponential electron distributions should give different spectra for the x-rays; we will present the differences between both, and emphasize the influence of the pulse profile on the spectra. Then we will briefly describe how the resulting x-ray spectrum could be used as a diagnostic for both the electron beam and the laser beam.

CP737, *Advanced Accelerator Concepts: Eleventh Workshop,*
edited by Vitaly Yakimenko

THOMSON SCATTERING SPECTRUM

Single electron spectrum from a uniform laser pulse profile

The power radiated per unit frequency and solid angle by a single electron moving in an ultraintense laser field can be described by the classical formula [7]

$$\frac{d^2I}{d\omega d\Omega} = \frac{e^2\omega^2}{4\pi^2 c}\left|\int dt\mathbf{n}\times(\mathbf{n}\times\boldsymbol{\beta})e^{i\omega(t-\mathbf{nr}/c)}\right|^2, \quad (1)$$

where e is the electron charge, ω the frequency, c the speed of light in vacuum, $\mathbf{n}$ a unit-vector pointing toward the observer, $\boldsymbol{\beta}$ the velocity of the electron divided by c, and $\mathbf{r}$ its position-vector.

It is necessary to know the electron orbit in order to solve for Eq. (1). If the electron is moving in a laser field $\mathbf{a}(z,t)$, then the orbit can be estimated analytically. Here $\mathbf{a} = e\mathbf{A}/mc^2$ is the normalized vector potential of the field, whose amplitude can be expressed in terms of the laser wavelength λ_0 and intensity I by $a_0 = 0.85\lambda_0[\mu m]\sqrt{I[10^{18}W/cm^2]}$.

Calculations for a uniform pulse of arbitrary polarization have been performed in Ref. [8]. In this case, the linearly polarized laser field is represented by: $\mathbf{a}(z,t) = \overline{a}(t)\cos k_0\eta\,\mathbf{e_x}$, where $\overline{a}(t) = a_0$ (uniform pulse) and $\eta = z+ct$ (the laser propagates toward $-\mathbf{e_z}$).

It is shown that for small field amplitudes ($a_0 \ll 1$), the electron emits light at the fundamental frequency $\omega_1 = \omega_0(1+\beta_0)/(1-\beta_0)$, where $\beta_0 = v_0/c$ ($\beta_0 > 0$) is the initial velocity of the electron along $\mathbf{e_z}$. The light is mostly emitted in the propagation direction, within a cone of angle $1/\gamma_0$ (with $\gamma_0^{-2} = 1-\beta_0^2$). For $\beta_0 \simeq 1$ (relativistic electron) we have $\omega_1 \simeq 4\gamma_0^2\omega_0$.

For large $a_0 \geq 1$ values, the electron motion becomes non-linear: in addition to the linear oscillations along the polarization direction of the laser field, it starts to gain longitudinal momentum and the resulting motion is the well-known "figure 8" pattern [7, 8]. The spectrum shows odds harmonics of the fundamental frequency, each of them being Doppler-shifted by a factor $1+a_0^2/2$ due to the longitudinal recoil of the electron.

The width of each harmonic is simply given by $\Delta\omega_n/\omega_n = n/N_0$, where n is the harmonic order and N_0 is the number of laser oscillations. In other words, the longer the interaction duration, the thiner the spectral peaks.

Spectrum from a non uniform laser pulse profile

We will represent a non-uniform laser pulse by denoting the pulse shape by $\overline{a}(t)$ (still normalized to a_0). For simplicity, we will restrict ourselves to the case of a purely counter-propagating laser pulse, with the electrons moving toward $\mathbf{e_z}$ ($\boldsymbol{\beta}_0 = \beta_0\mathbf{e_z}$) and the laser moving toward $-\mathbf{e_z}$ ($\eta = z+ct$). We will only consider the radiation emitted in the purely backscattered direction, i.e., $\mathbf{n} = \mathbf{e_z}$, as well as a lineary polarized laser pulse along $\mathbf{e_x}$.

The electron velocity in the case of an arbitrary laser field is given by [8]

$$\beta_x = \frac{a}{\gamma}, \tag{2}$$

$$\beta_y = 0, \tag{3}$$

$$\beta_z = \frac{h_0^2 - (1+a^2)}{h_0^2 + (1+a^2)}, \tag{4}$$

where $\gamma = (h_0^2 + 1 + a^2)/2h_0$ and $h_0 = \gamma_0(1+\beta_0)$. Within our geometry, the term $\mathbf{n} \times (\mathbf{n} \times \boldsymbol{\beta})$ in Eq.(1) simplifies to $-\mathbf{a}/\gamma$. It is convenient to make the change of variables $(z,t) \to (\eta = z + ct, \tau = t)$. Then the phase term becomes: $\psi = \omega(t - \mathbf{nr}/c) = (\eta - 2z)$. Since $d\mathbf{r}/dt = c(1+\beta_z)d\mathbf{r}/d\eta$, the coordinate z can be expressed as a function of η,

$$z(\eta) = z_0 + \frac{h_0^2 - 1}{2h_0^2}\eta - \frac{1}{2h_0^2}\int d\eta a^2(\eta), \tag{5}$$

where $h_0 = \gamma_0(1+\beta_0)$ and the constant of integration z_0 will be set to zero.

Then, we change the variables by noticing that $d\eta = c(1+\beta_z)dt$; since $\gamma(1+\beta_z)$ is a constant of motion, $\gamma(1+\beta_z) = \gamma_0(1+\beta_{z0})$ [8], Eq.(1) reduces to

$$\frac{d^2 I}{d\omega d\Omega} = \frac{e^2\omega^2}{4\pi^2 c^3 h_0^2}\left|\int d\eta a(\eta) e^{i\frac{\omega}{ch_0^2}(\eta + \int a^2(\eta)d\eta)}\right|^2 \tag{6}$$

To our knowledge, only Brau [9] attempted to solve this equation analytically for a non-uniform pulse profile. Unfortunately, the method used (stationary phase) fails to calculate the ends of the spectrum, and the absence of a stationary point makes the integral diverge. As a consequence, the most important part of the spectrum, i.e., the region where the scattered intensity is maximum, cannot be described. As the numerical calculation of Eq.(6) is straightforward, we will use this technique in the rest of the paper to investigate the effects of the finite laser time-envelope.

As it was already observed in [9], the time-profile of the laser gives rise to oscillations in the scattered spectrum. Indeed, the electron will first undergo small oscillations near the beginning of the pulse, where $\overline{a}(t) \ll a_0$, and emit light at the relativistic Doppler shifted-laser frequency ω_1. When the field amplitude increases, the electron is pushed backward, and its radiation undergoes a *classical* Doppler shift: the odd harmonics that are present if $a_0 \geq 1$ are downshifted by a factor $1 + a_0^2/2$. Then, when the field decreases back to zero, the electron radiates at ω_1 again. This radiation interferes with the radiation from the increasing part of the pulse, hence creating the oscillations in the spectrum. These are represented in Fig. 1 for the first harmonic only, for the case of a Gaussian profile with $a_0 = 1$, $\gamma_0 = 5$ and $N_0 = 7$ or 30. This shows that the number of oscillations scales like the number of wiggler periods.

The spectral broadening of each harmonic of order n extends from $n\omega_1$ to $n\omega_1/(1 + a_0^2/2)$ (we always assume that the electron interacts with all the pulse profile, i.e., the interaction length between the electron and the laser is the pulse length $L_0 = c\tau_0$); hence we can notice that it is possible to have an overlap between different harmonics. The

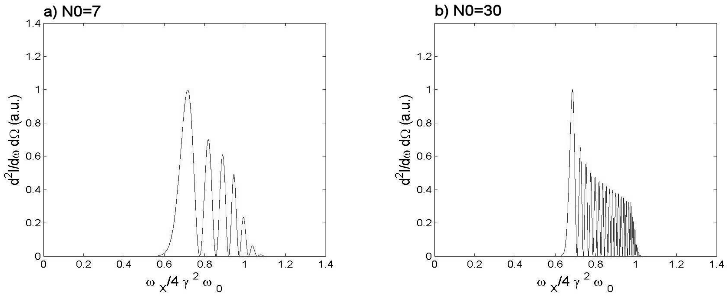

FIGURE 1. Spectrum of the first harmonic for a linearly-polarized laser pulse with a Gaussian profile and $a_0 = 1$, $\gamma_0 = 5$, $N_0 = 7$ (a) or 30 (b). The x-axis is normalized to the fundamental frequency $\omega_1 \simeq 4\gamma_0^2\omega_0$.

condition for an overlap of the $(n+2)^{th}$ harmonic on the n^{th} is $\omega_{n+2}/(1+a_0^2/2) \leq \omega_n$. This condition reduces to

$$a_0 \geq \frac{2}{\sqrt{n}}. \tag{7}$$

This shows that the higher harmonics will overlap first, and that even moderate ($\simeq 1$) values of a_0 are sufficient to start an overlap between the harmonics in the case of a non-uniform pulse profile. In particular, one can notice that *all* the harmonics of the spectrum will overlap with each other as soon as $a_0 = 2$. This is represented on Fig. 2 for $a_0 = 1.5$ and $a_0 = 2.1$. As expected, in the first case the high harmonics overlap up to the fifth with the third, and in the second case all of them overlap down to the first.

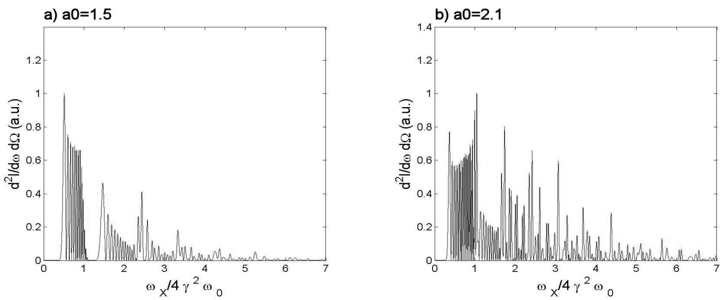

FIGURE 2. Spectrum for a linearly-polarized laser pulse with a Gaussian profile and $\gamma_0 = 5$, $N_0 = 7$ and $a_0 = 1.5$ (a) or 2.1 (b).

It is clear that such spectra are more difficult to analyse than the ones calculated from uniform laser pulses. As it will be demonstrated in the next section, additional complications arise when non ideal effects such as energy spread are taken into account.

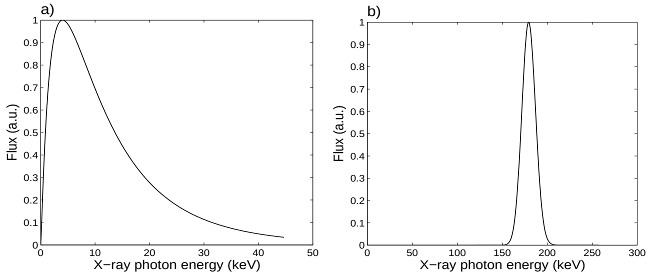

FIGURE 3. Expected x-ray spectra in the $a_0 \ll 1$ limit from: a) a broad electron distribution $f(\gamma) \propto exp[-\gamma/\gamma_0]$ with $\gamma_0 = 10$, and b) a narrow electron energy distribution $f(\gamma) \propto exp[-((\gamma-\gamma_0)/\Delta\gamma)^2]$ with $\gamma_0 = 196$ (100 MeV electron beam) and $\Delta\gamma = 6$; the laser wavelength is $\lambda_0 = 1.06\mu m$.

ELECTRON AND LASER BEAMS DIAGNOSTICS

Electron beam energy distribution

Laser-plasma-based accelerators can potentially produce two kinds of energy distributions: a low energy distribution, with an exponentially-decreasing distribution function as in the self-modulated regime[10], and a high-energy peak with a very narrow width, which is expected from colliding pulse injection experiments. The x-ray spectrum obtained from Thomson scattering should be very different between those two cases, i.e., narrow for a narrow energy distribution, and much broader for the exponential distribution.

The spectrum can be obtained from a convolution between the single-electron spectrum and the electron energy distribution function $f(\gamma)$ (with $\int_1^\infty f(\gamma)d\gamma = 1$),

$$\frac{d^2 I_T}{d\omega d\Omega} = \int d\gamma \frac{d^2 I(\gamma)}{d\omega d\Omega} f(\gamma). \tag{8}$$

It has been shown [11] that for an exponential energy distribution and $a_0 \ll 1$, the width of the peak emitted by each electron at the fundamental frequency ω_1 is very narrow, and can be approximated by a delta-function for the integration over γ. For a given energy distribution, the spectrum then simplifies to:

$$\frac{d^2 I_T}{d\omega d\Omega} = \frac{e^2}{16c} N_0 N_e a_0^2 \left(\frac{\omega}{\omega_0}\right)^{3/2} f(\gamma_{res}), \tag{9}$$

where N_e is the number of electrons and $\gamma_{res} \simeq \sqrt{\omega/4\omega_0}$ for relativistic electrons.

On the other hand, for a narrow energy peak, the x-ray spectrum should be peaked at the fundamental frequency. Fig. 3 shows the two expected spectra for a uniform laser profile ($\overline{a}(t) = a_0$), and for two characteristic energy distributions (exponential and narrow-peak).

The x-ray spectrum could hence provide useful information on the electron beam when cross-correlated with the electron energy distribution function. In the limit $a_0 \ll 1$, this might be used as an on-line, non-perturbative method to probe electron beams from storage rings.

Nonuniform pulse profile with energy spread

We have seen that in the non-linear regime where $a_0 \geq 1$, a non-uniform pulse profile should result in a very complex spectrum structure of overlapping peaks through a very wide range of frequencies. Adding an energy spread instead of purely mono-energetic electrons should cause enhanced broadening of these peaks and lead to a very broad spectrum.

We have performed numerical calculations of the convolution between a Gaussian energy distribution function for the electrons, $f(\gamma) = f_0 exp[-((\gamma - \gamma_0)/\Delta\gamma)^2]$, and the spectrum of a single electron for a non-uniform pulse profile as described by Eq. (6).

We used a relatively narrow (10%) width of the energy peak, with two values of laser intensity a_0=1 and 2. The resulting spectra are represented on Fig. 4, together with the corresponding spectra of a single electron. It is clear that the spectrum becomes strongly smoothed, and that the energy originally radiated inside narrow frequency peaks is now ditributed into a quasi-continuum of frequencies.

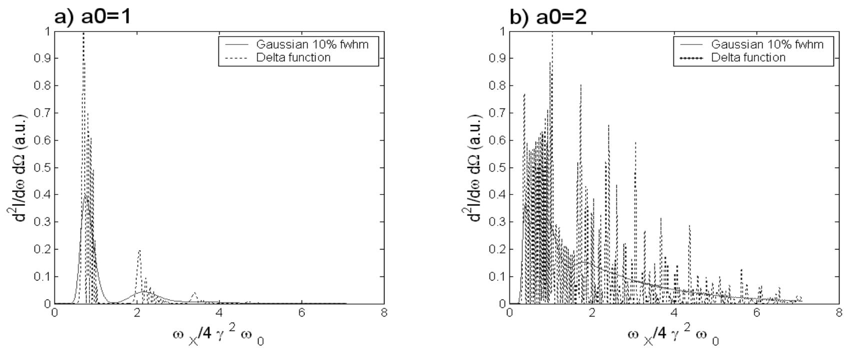

FIGURE 4. Spectra for a laser pulse with a Gaussian pulse shape and a_0=1 and 2. The corresponding spectra for single electron (delta-function energy distribution) are represented.

There are two main implications of the non-uniform laser profile with $a_0 \geq 1$ and a realistic electron beam with finite energy spread:

- For use of the scattered light as an ultrashort x-ray source, the laser profile and finite energy-spread effects will severely decrease the flux within a narrow bandwidth that one might expect from simple estimates, and smooth all the main characteristics of the spectrum;
- For use as a diagnostic, this should make it more difficult to extract information about the electron beam from the x-ray spectrum.

However, it should be emphasized that the low cut-off frequency $\omega_1/(1+a_0^2/2)$ allows a measurement of the laser a_0 parameter. Indeed, the a_0 parameter, although of extreme importance for all applications, is usually difficult to determine as the focal spots at high energies are always strongly aberrated. A significant fraction of the light then occurs far outside the diffraction-limited surface, which makes it almost impossible to determine an accurate value for the intensity at the focus. Note that this method should especially be useful for the $a_0 \simeq 1$ regime (i.e., $I \simeq 10^{18}$ W/cm^2 for typical wavelengths).

CONCLUSION

In summary, we have demonstrated the effects of non-uniform laser pulses together with a finite energy spread of the electron beam. It was demonstrated that using a laser with a large a_0 and a finite time-profile (i.e., in the configuration where the interaction length is the pulse length $L_0 = c\tau_0$) could result in a severe broadening and overlap of the harmonic peaks of the x-ray spectrum. Although determining electron bunch characteristics from such a spectrum might become difficult, it could still be used as a way to measure the laser strength parameter a_0.

ACKNOWLEDGMENTS

This work supported by DoE, DE-AC03-76SF0098.

REFERENCES

1. Schoenlein, R. W., Leemans, W. P., Chin, A. H., Volfbeyn, P., Glover, T. E., Balling, P., Zolotorev, M., Kim, K. J., Chattopadhyay, S., and Shank, C. V., *Science*, **274**, 2361 (1996).
2. Leemans, W. P., Schoenlein, R. W., Volfbeyn, P., Chin, A. H., Glover, T. E., Balling, P., Zolotorev, M., Kim, K. J., Chattopadhyay, S., and Shank, C. V., *Phys. Rev. Lett.*, **77**, 4182 (1996).
3. Esarey, E., Sprangle, P., Krall, J., and Ting, A., *IEEE Trans. Plasma Sci.*, **24**, 252 (1996).
4. Nakamura, K., Fubiani, G., Geddes, C. G. R., Michel, P., van Tilborg, J., Toth, C., Esarey, E., Schroeder, C. B., , Leemans, W. P., and Uesaka, M., "Laser triggered injection of electrons in a laser wakefield accelerator with colliding pulse method," in *Advanced Accelerator Concepts 2004*, American Institute of Physics, New York, 2004, AIP Conference Proceedings.
5. Esarey, E., Hubbard, R. F., Leemans, W. P., Ting, A., and Sprangle, P., *Phys. Rev. Lett.*, **79**, 2682 (1997).
6. Fubiani, G., Esarey, E., Schroeder, C. B., and Leemans, W. P., *Phys. Rev. E*, **70**, 016402 (2004).
7. Jackson, J., *Classical Electrodynamics (3d ed.)*, Wiley, 1999, p. 676.
8. Esarey, E., Ride, S. K., and Sprangle, P., *Phys. Rev. E*, **48**, 3003 (1993).
9. Brau, C., *Phys. Rev. Spec. Topics Accel. Beams*, **7**, 070201 (2004).
10. Leemans, W. P., van Tilborg, J., Faure, J., Geddes, C. G. R., Tóth, C., Schroeder, C. B., Esarey, E., , and Fubiani, G., *Phys. Plasmas*, **11**, 2899 (2004).
11. Catravas, P., Esarey, E., and Leemans, W. P., *Meas. Sci. Technol.*, **12**, 1828 (2001).